CHAPTER 14

Recupera exoskeletons

Martin Mallwitz[a,e], **Michael Maurus**[a,e], **Shivesh Kumar**[a],
Mathias Trampler[a], **Marc Tabie**[a], **Hendrik Wöhrle**[a,d], **Elsa A. Kirchner**[c],
Henning Wiedemann[b], **Heiner Peters**[a], **Christopher Schulz**[a],
Kartik Chari[a], **Ibrahim Tijjani**[a], **and Frank Kirchner**[a,b]

[a]Robotics Innovation Center, German Research Center for Artificial Intelligence (DFKI GmbH), Bremen, Germany
[b]Working Group Robotics, University of Bremen, Bremen, Germany
[c]Institute of Medical Technology Systems, University of Duisburg-Essen, Duisburg, Germany
[d]Institute of Communication Technology, Dortmund University of Applied Sciences and Arts, Dortmund, Germany

14.1 Introduction

The development of exoskeletons as an active external support structure for the human body has made significant progress in recent decades thanks to miniaturization and digitalization. The decisive factor for acceptance and handling is mechanical transparency [1] for the user, in the sense of perceived restriction of movement. This applies to the application of the exoskeleton as a power assistance, as an input device for remote control or as a robotic rehabilitation device [2].

14.1.1 Motivation for series-parallel hybrid design

Building a robotic support structure around humans, which is not perceived as restrictive, places high demands on the ergonomics of the kinematic setup. Human joints are complex structures in terms of their mobility and can often only be approximated with rigid mechanics by combinations of rotational and linear joints. In addition to the bony skeletal structure, they consist of cartilage, capsules, tendons, ligaments and muscles. In order to adequately represent the shoulder joint, at least three, preferably five, rotational mechanical joints have to be combined. The joint axes often cannot be mapped directly, since the construction space is limited by the human body. Collisions of the mechanics with the human body must be prevented during motion. The use of parallel kinematics can separate the main pivot

[e] The two authors contribute equally to the work.

point of a mechanism from the drive axis, thus making optimum use of the installation space. At the same time, the movement can be restricted in a defined way. This is achieved by positively guided movement of numerous links of the mechanism. The advantages of parallel kinematics include more freedom for installing the actuators, high stiffness and a good dynamic behavior, but it increases the number of moving components and the effort in modeling and controlling the system. Their application must therefore be justified. A combination of serial and parallel kinematics in many cases leads to very good overall results in terms of motion space, force transmission and installation space. This design philosophy forms the basis of RECUPERA exoskeletons, as shown in Fig. 14.1.

14.1.2 Application scenarios

The RECUPERA exoskeletons were developed as a training device for stroke rehabilitation [3] and modified for the purpose of teleoperation.

14.1.2.1 Rehabilitation scenario

Exoskeletons and here especially active exoskeletons can be used for the rehabilitation of patients, e.g., after a stroke [4]. Compared to the use of exoskeletons for the compensation of paralysis, especially after spinal cord damage, this application is not yet very well established. However, there are some studies showing that robot-assisted rehabilitation shows great effects [5]. Active exoskeletons are able to introduce forces into the patient's body and thus support them in their movements or make them possible in the first place. The support adapted to the specific requirements of the patient is called assist as needed [6].

14.1.2.2 Teleoperation scenario

Exoskeletons can also be applied for teleoperation. Teleoperation in general means the remote control of a robotic system [7,8]. In our case, we understand teleoperation as the remote control of a robotic system equipped with one or two manipulators. Teleoperation can be a very useful tool when an on-site presence is either too expensive (e.g., space exploration missions), too dangerous (e.g., search and rescue) or not applicable at all (e.g., deep sea). The exoskeleton used has to be easily controllable and mapped to the target system with respect to the application. For example, when teleoperating a humanoid robot, it is preferable to map not only the hand positions but additionally the elbow positions to improve operator immersion and

(a) Upper-body system   (b) Full-body system
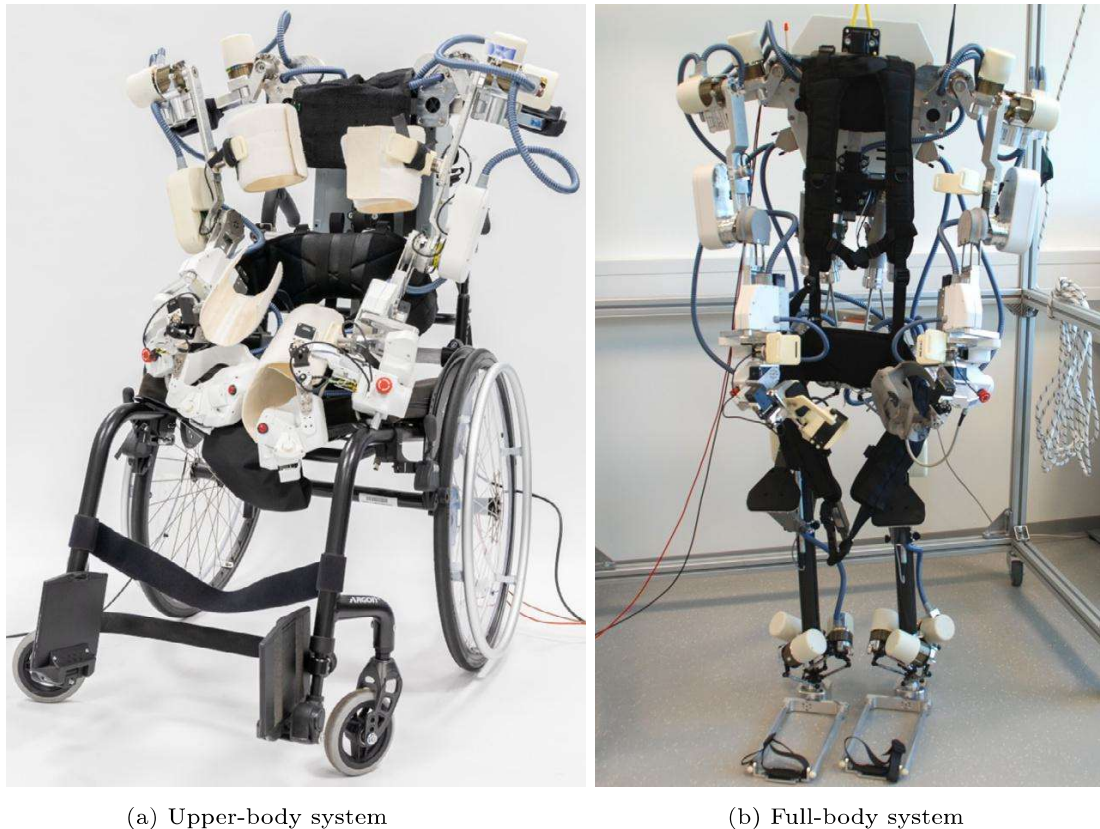
Figure 14.1   The RECUPERA upper-body exoskeleton is a part system of the full-body exoskeleton mounted on wheelchair.

mapping of the workspaces of the two different systems. Active exoskeletons also have the advantage of being a haptic interface [9]. This means that it is possible to give force feedback to the operator from forces occurring in the controlled target system and measured at force-torque sensors in order to provide better support, especially for remote manipulation tasks.

Organization

In this chapter, we present the RECUPERA full–body exoskeleton and the RECUPERA upper–body exoskeleton subsystem. Section 14.2 describes the mechatronic components and explains the modular concept in terms of mechanical sub-mechanisms and decentralized control units. Section 14.3 details the kinematic modeling, the dynamic model of the exoskeleton and the 3-stage control design and their relation to the application. The achieved results of the rehabilitation application and teleoperation are discussed in Section 14.4. Finally, a summary and outlook is provided in Section 14.5.

14.2 Mechatronic system design

The RECUPERA exoskeleton was developed in order to provide a support and training device for stroke patients. In cooperation with a medical device manufacturer, the general requirements for actuation, range of motion (ROM), degrees of freedom (DOF), safety and application scenario were defined. The exoskeleton was designed as a safe, lightweight and modular system in both the mechanical and electrical sense.

Two configurations were built to be able to perform the training application both in sitting and standing position. The first configuration includes the arm structure and is mounted on a wheelchair, while the second is a full-body system with active hip, knee, ankle, and spine to support its own weight (see Fig. 14.1).

The RECUPERA exoskeleton is also used to remotely control another robot. The target system is the humanoid robot RH5 MANUS [10], which was designed to support a human in assembly tasks. This includes complex gripping tasks of objects designed for humans. The requirements change noticeably due to the new application, where an input device for grasping with force feedback is needed.

The main changes are the addition of the wrists with two active DOF, larger torques and forces acting on the human and robotic arms, and new possibilities for fine manipulation with the human hand.

14.2.1 Mechanical design

In order to adapt the exoskeleton to the needs and movement spaces of humans, serial and parallel kinematics were combined and equipped with the institute's own drives. The system is thus a modular serial–parallel hybrid robot with numerous adaptation options, components of which are presented below. Fig. 14.2 gives an overview about sub-mechanisms and its used actuators, as Table 14.1 shows the ROM.

14.2.1.1 Actuators

Due to the lack of suitable commercial offers, DFKI has developed its own drives for the robotic systems for a torque range of 3 Nm to 500 Nm (in case of rotary drives) or force range of 1 kN to 5 kN (for linear drives). Two types of these drives are used in the RECUPERA exoskeleton along with some commercial servos and are presented below.
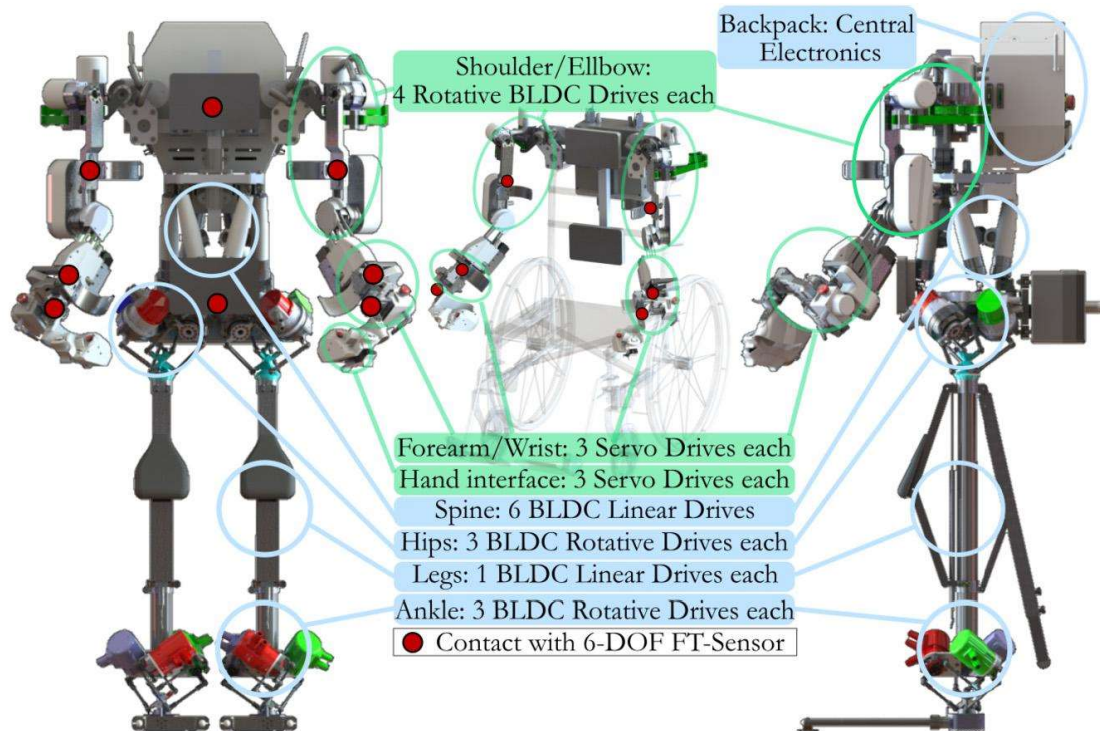
Figure 14.2 CAD overview of the robotic systems. Components marked in green are part of both systems, components marked in blue belong exclusively to the full-body exoskeleton.

DFKI rotative drives

The arms and ankles, as depicted in Fig. 14.2, are equipped with drives consisting of a combination of a BLDC installation kit from TQ-SYSTEMS and a HARMONICDRIVE gearbox. This provides a high power density and low backlash (< 1 arcmin) drive unit. Magnetic off–axis high–resolution position sensors MU from iC-HAUS are used for the rotor commutation and the detection of the absolute joint position.

DFKI linear drives

These drives essentially consist of a combination of a TQ-SYSTEMS BLDC motor and a ball screw. The motor directly drives the nut of the ball screw. The spindle itself is stationary, which is particularly advantageous for long spindles in combination with high speeds. The commutation and incremental measurement is done with the help of an iC-HAUS MU sensor. For absolute measurement, a linear potentiometer is used in the leg drives and a rope potentiometer in the STEWART-GOUGH PLATFORM drives. The backlash in the drives is (< 0.01 mm).

Table 14.1 Overview of range of motion.

Body part	Motor	Movement	Range
Shoulder	RD 50x8	Abduction / Adduction	–87° to 40°
		Ext. Rotation / Int. Rotation	–40° to 75°
		Flexion / Extension	–170° to 30°
Elbow	RD 50x8	Flexion	0° to 145°
Forearm	DY XH540W	Pronation / Supination	–88° to 88°
Wrist	DY XH430W	Palmar Flexion / Dorsiflexion	–43° to 43°
		Radial abduction / Ulnar add.	–20° to 40°
Spine	RD 38x8	Forward / Backward	–0.143 m to 0.122 m
		Left / Right	–0.153 m to 0.153 m
		Up / Down	–0.056 m to 0.057 m
		Flexion / Extension	–33° to 33.5°
		Lateral Bending	–33° to 33°
		Rotation	–87° to 87°
Hip	RD 70x10	Flexion / Extension	–20° to 37°
		Adduction / Abduction	–15° to 35°
		Lateral Rotation / Medial Rot.	–20° to 37°
Leg	RD 38x12	Up / Down	0.46 m to 0.71 m
Ankle	RD 50x8	Dorsi Flexion / Plantar Flexion	–20° to 37°
		Eversion / Inversion	–15° to 35°
		Adduction / Abduction	–20° to 37°

Commercial servos

DYNAMIXEL–X servo drives from ROBOTIS are used in the forearm for pronation and supination and in the wrist. They consist of a BLDC motor combined with a spur gear and are equipped with their own electronics including a position sensor. MKS–DS95 model servo drives are installed in the hand interface and actuate the fingers.

14.2.1.2 Sub-mechanism modules

Depending on the function and range of movement in the overall system, the sub-mechanisms are designed and combined to form a complete system. Fig. 14.3 gives a detailed view of the individual mechanisms.

Table 14.2 Overview of used actuators with following abbreviations: TQ-SYSTEMS ROBODRIVE(RD), HARMONICDRIVE (HD), Muliturn (MT), rotative (rot), linear (lin), ROBOTIS DYNAMIXEL (DY).
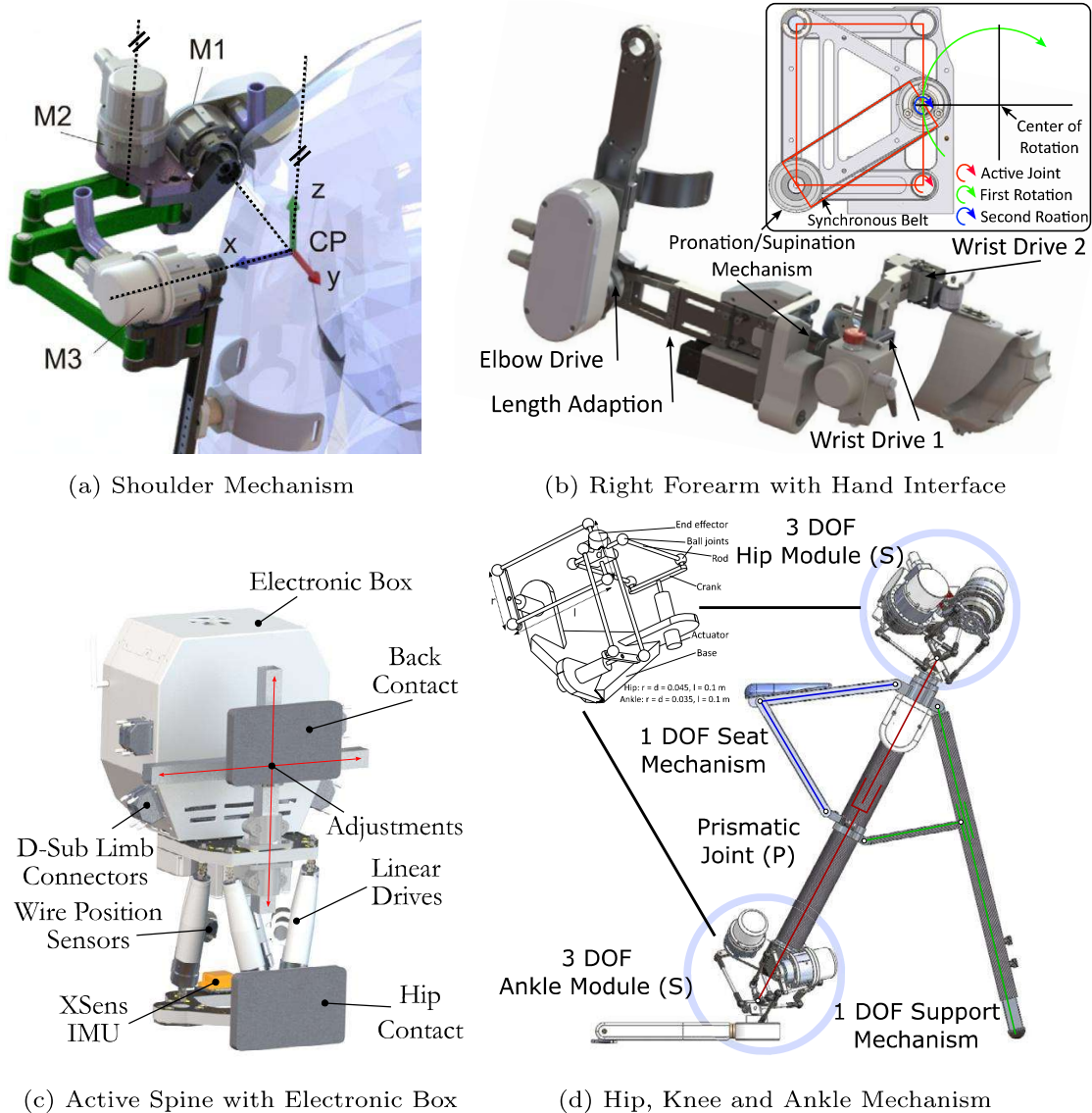
Motor	Type	Gear	Torque	Max Speed	ROM
RD 50x8	rot	HD CPL14A-50/100:1	18/28 Nm	700/350 °/s	MT
RD 70x10	rot	HD CPL25-160:1	92 Nm	132 °/s	MT
DY XH540W	rot	152.3:1	7.1 Nm	420 °/s	MT
DY XH430W	rot	353.5:1	3.4 Nm	180 °/s	MT
MKS-DS95	rot	Metal Gear	0.3 Nm	1132 °/s	360°
RD 38x12	lin	Ballscrew FBR 8x2	570 N	266 mm/s	130 mm
RD 38x12	lin	Ballscrew FGR 8x2	570 N	266 mm/s	420 mm

Shoulder mechanism

The human shoulder joint is a complex structure that allows a very high degree of mobility in six DOF. The RECUPERA shoulder mechanism simplifies this joint into a ball-and-socket joint that allows rotation in three axes, as depicted in Fig. 14.3a. This is an almost exact replica of the human shoulder joint, as the connection to the exoskeleton is not rigid and thus compensates for missing translational movements. It consists of a serially-connected chain of joints, the middle joint of which is a parallel-guided mechanism. The first joint in the chain allows for abduction and adduction, the second for internal and external rotation and the third for anteversion and retroversion of the arm. All three joints are arranged so that their axes of rotation intersect in the shoulder of the user. In order to increase the range of movement and to avoid a collision with the user, the second shoulder joint is designed as a planar six-bar double parallelogram mechanism. This allows the drive to be placed outwards without having the same axis of rotation. Two coupling joints are fixed to the back structure so that the end-effector rotates around an ideal point.

Elbow and forearm

The forearm mechanism has been extended by two active DOF in the wrist and the torques of the drives have been increased to allow adequate force feedback. The elbow drive is an RD 50x8 BLDC motor with a 50:1 re-

(a) Shoulder Mechanism

(b) Right Forearm with Hand Interface

(c) Active Spine with Electronic Box

(d) Hip, Knee and Ankle Mechanism

Figure 14.3 Sub-mechanism modules.

duction gear. The pronation and supination of the forearm is enabled by a parallel coupling gear inspired by the Harmony exoskeleton [11]. Fig. 14.3b shows the entire forearm and the detailed kinematics of the forearm is depicted in Fig. 14.6. At the lower lever of the parallelogram, the drive turns the entire mechanism. In the process, the left toothed belt pulley is also rotated and the rotation is transmitted to the output by means of a toothed belt, thus performing a movement around the ideal pivot point. Symmetrical selection of the swing arms results in an exact circular movement and power transmission in a ratio of 1:1. Two mechanical stops limit the total range of movement to 176°. This prevents that the singularity is reached, where all joints of the parallelogram are arranged in a line. The subsequent

joints of the wrist are arranged as a serial chain. The first joint allows radial abduction and ulnar adduction, the second palmar flexion and dorsiflexion.

Hand interface

The rehabilitation hand interface is designed as a curve guided coupling mechanism with one DOF and an end-effector movement range of 90°. The mechanism is driven by an MKS-DS95 servo with 0.3 Nm and can apply a maximum gripping force of 5 N. A Honeywell FSG15N force sensor is connected between the gear and the output and is used to control the gripping force.

The teleoperation hand interface (see Fig. 14.3b) was designed to enable an operator to remotely control a robot, with a focus on grasping tasks. For this, it features three surfaces with force feedback to create the sensation of grasping an object via a surrogate motion.

The surfaces are mounted on linear sliders with a stroke of 20 mm and are driven by an MKS-DS95 servo motor each. The resistive force, applied by the operator's fingers, is measured by Honeywell FSG15N force sensors. One slider corresponds to the index finger, one to the thumb and one to middle, ring and little finger. This allocation was chosen since in many tasks, the last three fingers are often used together, whereas thumb and index finger are used more individually. Since the sliders are driven by the servos via levers, the maximum feedback force is not constant throughout the ROM, but varies between 14 N and 20 N.

In addition to the sliders with gripping surfaces, each hand interface features two buttons, a joystick with integrated push button and an emergency stop. The hand interface is ergonomically shaped and provides a hand rest to assist the operator in keeping a relaxed hand posture.

Torso structure

The torso design utilizes the advantages of a parallel kinematic machine in terms of the force-to-weight ratio and the inherent limitation of the ROM. The Stewart–Gough Platform in Fig. 14.3c consists of six variable length drives operating in parallel. It allows three rotational and three translational motions and is classified as 6-[UPS] mechanism, with the underlined letter indicating the active joint. It is highly mobile, highly dynamic and has high rigidity. The linear spindle drives are shown in Section 14.2.1.1 and are equipped with an additional absolute linear sensor and mechanical limits. All drive electronics are based on the baseplate and are

unified as Actuator Control Unit, see Section 14.2.2.1. The movement of the back assists in standing up and sitting down and increases the reach of the arms. The electronic box is mounted on the top plate of the mechanism. An XSENS MTI300 inertial sensor is also mounted on the base plate of the hip joint connection.

Hip and ankle

The hip and foot are equipped with a specially developed almost spherical parallel mechanism (ASPM) that acts as a 3 DOF swivel joint. For this purpose, three rotative drives each drive the end-effector via a spatial quadrilateral consisting of a coupling rod with two ball pivots. In the end-effector, the quadrilaterals are perpendicular to each other and intersect at their centers. In mechanism theory, the ASPM is classified as a PKM of type 3-[R–[2-SS]] [12,13]. Mechanical end stops limit the three actuators and thus also the overall mechanism. A special feature is the equal distribution of the tension within the mechanism; due to the ball heads, only compression and tension forces are transmitted via the coupling rods. A force acting in the direction of the axis of rotation is absorbed by the bearing without active torque.

Knee joint

The legs of the exoskeleton cover approximately the full human ROM with 7 DOF fully actuated kinematics. Instead of a usual S-R-S architecture, in which a spherical joint is used to actuate the hip and ankle joint respectively and a rotational joint is used in the knee, the knee joint used here is replaced by a prismatic coupling between the hip and ankle joint. The resulting S-P-S architecture significantly reduces the bending stresses occurring in the leg structural components. Furthermore, the legs have additional passive kinematics in the area of the knee joints, which unfold from a certain shortening of the prismatic actuator. This serves to unfold an additional support as well as a seat structure in which the wearer of the exoskeleton can rest without the actuators having to utilize any electrical power (Fig. 14.3d). The unfolding threshold on the prismatic actuator was chosen such that the passive kinematics remain closed during a normal walking pattern and only unfold when the user flexes the knees further. The knee mechanism is actuated by a linear actuator consisting of a BLDC motor and a ball screw. For sitting and standing, the 3 DOF hip and ankle drives are used additionally. With the linear actuator force capability provided in Table 14.2, the two legs can apply a total force of 1120 N.

With a total weight of the exoskeleton of 42 kg, an additional weight of up to approximately 70 kg can be supported by the leg design in an upright posture.

14.2.1.3 Safety aspects

Safety in the use of an exoskeleton plays a fundamental role in order not to endanger the user. For the mechanical design, this essentially means limiting the forces and ROM of the robot. In order to maintain the dynamics and freedom of movement of the user, a negotiation process is necessary. In the RECUPERA exoskeleton, the drives were designed according to these principles and have integrated movement-limiting mechanical stops. Additionally, in the joints with high DOF such as the back, hips and ankles, the use of parallel kinematics provides intrinsic movement limitation. The human contacts to the exoskeleton are not rigid, but designed with Velcro. The back connection offers enough freedom to compensate for any misbehavior of the robot.

14.2.1.4 Interface with human

The upper-body exoskeleton is connected to the human at three contact points per arm and at two contact points in the back. The contacts on the upper arm, forearm and hand interface are equipped with 6-axis ATI NANO25 force/torque sensors and can thus measure the forces that occur between the exoskeleton and the human. In the full-body exoskeleton, 6-axis ATI NANO25 sensors are also installed in the contact points on the back and hips. A loop in the foot mechanism enables contact with the human foot. The hip and back contacts are realized by straps with quick-release fasteners, the contact in the upper arm by Velcro fasteners. Fig. 14.2 documents the position of the contacts and their sensory equipment.

14.2.1.5 Adaption to different human sizes

The exoskeleton is designed for people with an approximate body height of 1.6 m to 1.9 m. The necessary adaptation options are provided in the shoulder, arms, back and leg structures. The upper arm length is adjustable by 55 mm, the forearms have a possible length adaptation of 50 mm, as well as two different length elbow adapters that allow for an additional extension of 50 mm. The wrist can be adjusted by up to 15 mm horizontally and vertically, and the hand interface can be moved forward by 13 mm. The shoulder can be adjusted in height (79 mm) and width (130 mm). In addition, the STEWART−GOUGH PLATFORM and the height of the legs

can be adjusted to a defined starting level within a height of 100 mm. But this takes affect to the possible task space.

## 14.2.2 Electrical and electronic design

The electrical and electronic design of both the wheelchair and the full-body exoskeleton is based on a hybrid centralized-decentralized control scheme. Fig. 14.4 shows an overview of all actuators and the underlying network structure (see also Section 14.2.2.1 for details). The control on the actuator level is performed in a decentralized manner and provides real-time capabilities to support a multi-level safety strategy. Both the mid- and high-level controls are computed in the central processing system of the exoskeleton (see Fig. 14.4 and Section 14.2.2.2). They provide complex functionality, such as kinematics/dynamics computations and functions to interact with the user.

14.2.2.1 Decentralized actuator-level controllers

Every actuator is controlled by a dedicated modular Actuator Control Unit (ACU) which is placed close to the corresponding actuator. The ACUs are self-designed and have been developed to specifically control BLDC motors. An ACU typically contains three separate subunit PCBs: one PCB for power electronics, one for data acquisition and communication and one PCB for computing. Multiple different ACU PCB subunits can be combined in order to fulfill specific requirements of each actuator. Table 14.3 shows an overview of the configurations used in the RECUPERA exoskeleton. The control and communication functionality is realized using a dedicated hardware design in the Xilinx XC6SLX45 Spartan 6 FPGA on the computing PCB subunit. The used controller is implemented as a cascaded position–velocity–current PID algorithm (see Section 14.3.3.1). Every ACU is supplied with two different voltages. For the motor phases, a voltage of 48 V is used, while 12 V is used for the computing and communication part. Both voltages and the related currents are continuously monitored by the FPGA. For safety reasons, the FPGA implements a configurable, firmware-based fuse. Additionally, each ACU contains a hardware fuse.

14.2.2.2 Central electronics for mid and high level control

The central electronic system of the exoskeleton is located in a backpack. It contains all components that are required for the power supply, mid-
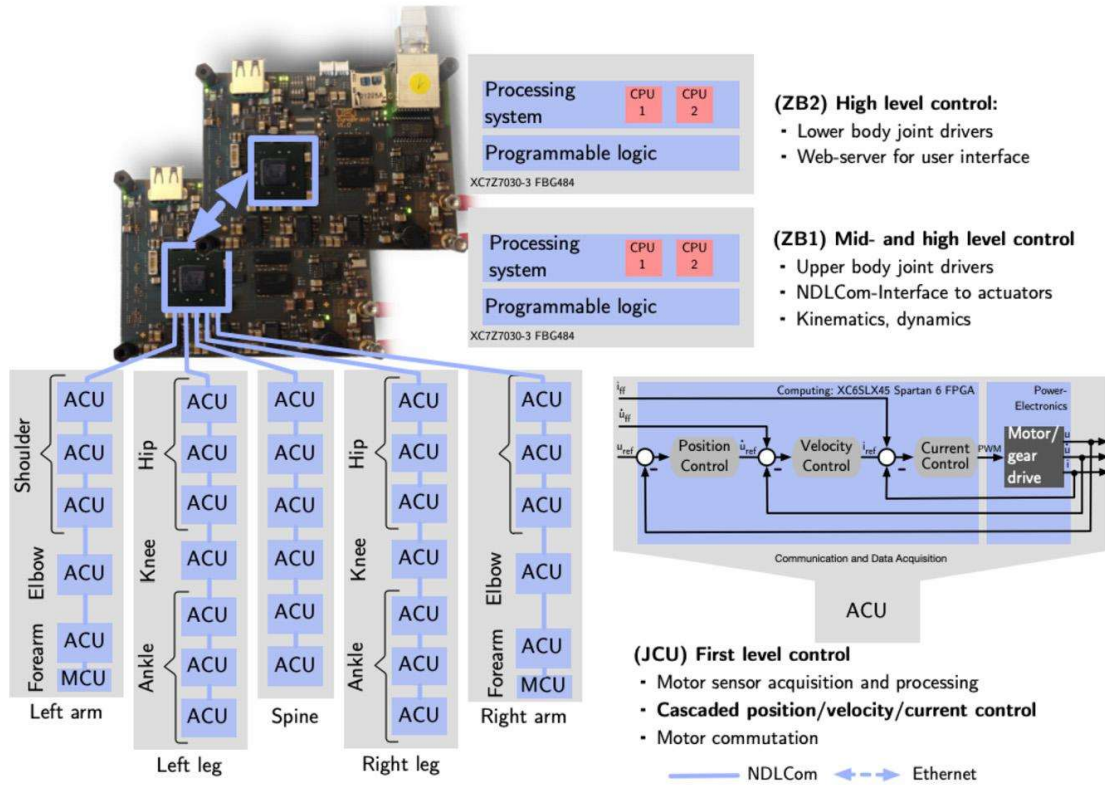
Figure 14.4 The exoskeleton is controlled by two central systems, called ZynqBrain (ZB), and a network of decentralized Actuator Control Units (ACU) for motor control. Each motor is controlled locally by an adjacent ACU. The distributed ACUs are connected via an NDLCom network [14]. Bottom right: cascaded actuator-level control architecture implemented on the FPGA of each ACU; u is the angular position, $\dot{u}$ is the angular velocity and i is the motor current. The reference values are provided by the mid-level control on the ZBs. All ACUs continuously send telemetry status data to ZB1 with 1 kHz using the NDLCom network.

and high-level control, software for the user interface, communication and networking as well as safety features like a wireless emergency switch. The main computing system consists of two dedicated Pico-ITX PCBs (70×100 mm) called *ZynqBrain*. It contains a Xilinx Zynq ZC7030 [16] System on Chip. A ZC7030 consists of two sections: a Processing System (PS) (which is a dual-core ARM Cortex-A9 CPU running at 1 GHz) and a Programmable Logic (PL) section. Furthermore, each ZynqBrain contains 512 MB DDR3 SD-RAM [17]. For dedicated communication with the ACUs, each ZynqBrain contains five duplex high-speed and low–voltage differential signaling (LVDS) interfaces (see also [18]).

Table 14.3 Configurations of the Actuator Control Units (ACU). Each ACU consists of zero or more PCBs for **P**ower electronics, **D**ata acquisition and communication, **C**omputation or **M**icrocontroller. To control a motor, it senses the motor position via iC-MU [15] **A**bsolute encoders or **R**elative encoders (Hall sensors). In addition, **L**inear potentiometers (WayCon) or draw **W**ire sensors (WayCon) are used for linear drives to sense the length.

	Location	ACU PCBs	Drive Unit	Sensors
Upper-body	Shoulder	P, D, C	RD 50x8–28	2xA
	Elbow	P, D, C	RD 50x8–14	2xA
	Forearm	D, C, M	Dy XH540W	2xA
			Dy XH430W	1xA
Lower-body	Spine	P, D, C	RD 38x12	A, W
	Hip	P, D, C	RD 70x10–160	A, R
	Knee	P, D, C	RD 38x12–2	A, R, L
	Ankle	P, D, C	RD 50x8–100	2xA

14.2.2.3 Power management

The DFKI's own Central Power Management Board (CPMB) serves as internal power supply and battery management. This allows the entire system to be supplied with the required voltages. The central computing unit is operated with 5 V, the decentralized ACU with 12 V for logic circuit and 48 V for power electronics. The CPMB can switch between an external power supply and a battery, as well as perform its charging function. Two additional voltage converters are located in the elbow and supply the DYNAMIXEL-X motors with a 12 V voltage separate from the logic voltage, as well as the model servos in the hand interface with 6 V. In the full–body system, the individual assemblies' arms, legs and the back can be switched on and off with two programmable electrical fuses and their power consumption can also be monitored. A more detailed description can be found in [18].

14.2.2.4 Safety aspects

To ensure safe operation of the exoskeleton, safety mechanisms were designed on three levels. The 48 V voltage supply for the motor power can

be switched off externally on both systems by means of emergency buttons on the arms, hand interface and on the full-body system on the back. A wireless emergency button operated by an external person and a foot pedal for the user provide the same functionality. Hard and soft limits for position, speed and current are specified at the decentralized ACU level and are decoupled from the mid and high software levels. When the hard limits are exceeded, this also causes the 48 V voltage to be interrupted. The soft limits are used as a control value limit and in the case of the position, exceeding the limit is prevented by moving in the opposite direction. On the software level, as a third element, there are further setpoint limits that cannot be exceeded.

14.3 Modeling and control

In this section, we present the kinematic and dynamic modeling of the possible exoskeleton configurations, the control architecture and software design for various rehabilitation therapies and teleoperation.

14.3.1 Modular robot description models

In its application, the RECUPERA exoskeleton is not only controlled in terms of position, but also based on forces and torques. For this purpose, the dynamic parameters of mass, center of gravity, moments of inertia and axes of rotation as well as their orientations of the individual robot links are required. The values can partly be determined experimentally or can be extracted from the CAD model. This is done with the SW2URDF tool [19]. To do this, the robot must be divided into the link-joint structure. Coordinate systems are assigned to the links and joint axes from origin to end-effector. The SW2URDF tool reads the values calculated in the CAD software, converts them into the Universal Robot Description Format (URDF) and links them to the exported meshes in STL data format.

The commissioning of a complex robotic system requires functioning sub-assemblies. Troubleshooting the entire system is complex and time-consuming due to the numerous possible errors on the hardware and software side. It makes sense, if possible, to commission and test individual sub-assemblies. Also, if there is a need to combine sub-assemblies in different ways, the advantage of a modular structure comes into play. Fig. 14.5 shows an overview of the different sub-assemblies used, which
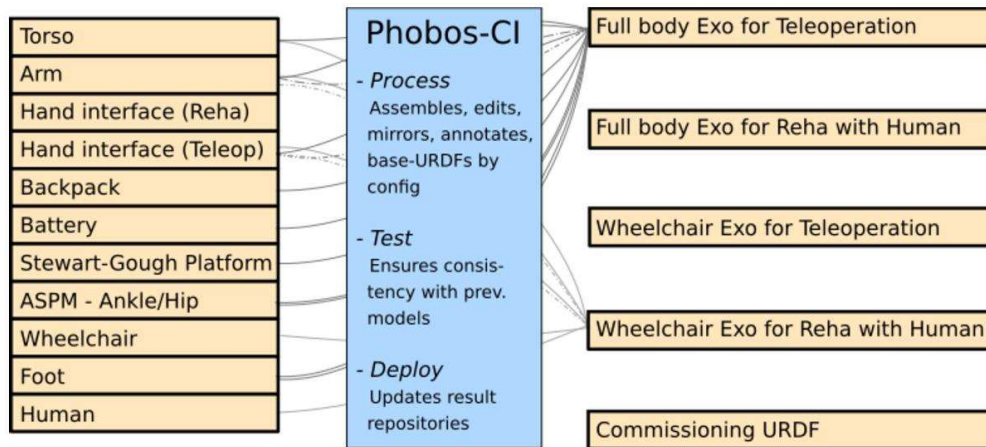
Figure 14.5 Overview of the exported (left), processed and used models (right). The PHOBOS-CI used to process the models is explained in Chapter 17.

are maintained using a Continuous Integration (CI) pipeline (see Chapter 17). Using this CI during the commissioning the various models are held consistent with each other.

14.3.2 Kinematics and dynamics

RECUPERA exoskeleton is a highly complex series–parallel hybrid mechanism with 34 DOF, where 24 DOF are actuated with parallel submechanism modules. Overall, the exoskeleton can be seen as a tree-type composition of 5 series–parallel hybrid submechanisms involving 2 legs, 2 arms and a torso. Hence, the loop closure function (LCF) of the overall system can be composed by combining the LCF of the 5 individual sub–assemblies.

Analytical LCF of RECUPERA arm

The RECUPERA exoskeleton arm is a 7 DOF series–parallel hybrid mechanism which contains a double parallelogram linkage at the shoulder joint and a parallelogram linkage in wrist joint (see Fig. 14.6 for its schematic and topological graph). The loop closure function of the parallelogram–like linkages can be composed from the mimic joint definition in URDF [20]. We choose an identical set of independent (γ) and active (u) joints from their topological graph shown with red edges ($J_{100,200}$, $J_{200,232}$, $J_{300,400}$, $J_{400,500}$, $J_{500,511}$, $J_{600,700}$, $J_{700,800}$). The spanning tree joints (excluding the loop joints shown by dotted blue edges) are collected in tree joint position
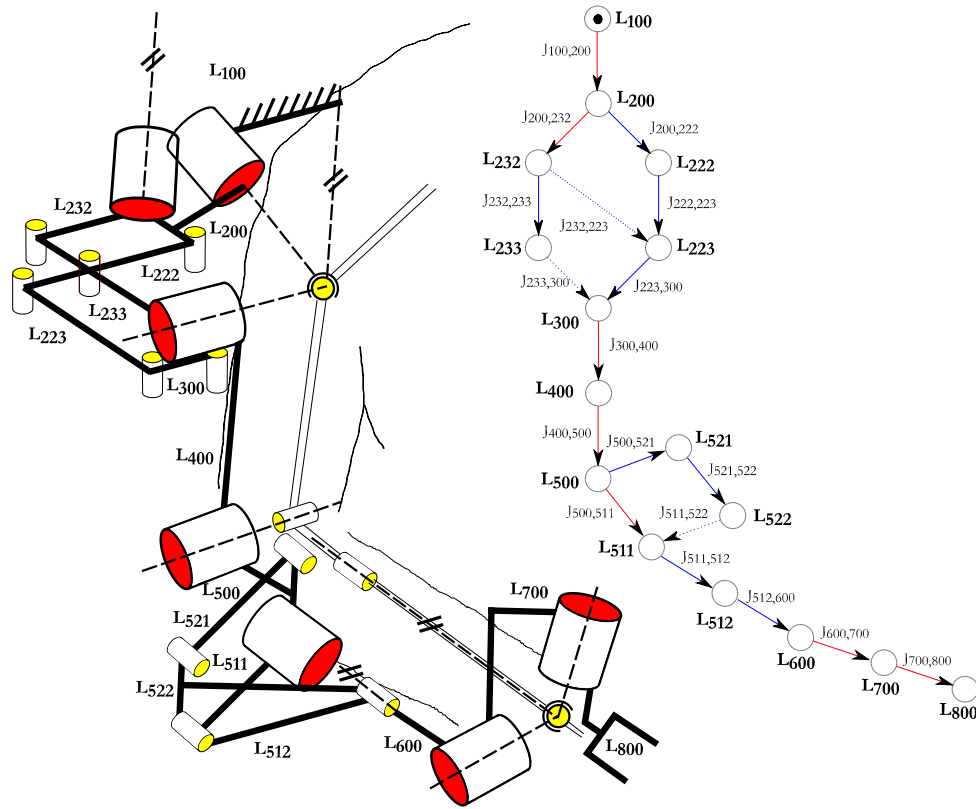
Figure 14.6 Single arm schematic and its topological graph.

vector q and its relation with γ, i.e., LCF (γ), is shown in Eq. (14.1).

$$
q = \begin{bmatrix} q_{100,200} \\ q_{200,222} \\ q_{222,223} \\ q_{223,300} \\ q_{200,232} \\ q_{232,233} \\ q_{300,400} \\ q_{400,500} \\ q_{500,521} \\ q_{521,522} \\ q_{511,522} \\ q_{500,511} \\ q_{511,512} \\ q_{512,600} \\ q_{600,700} \\ q_{700,800} \end{bmatrix} = \begin{bmatrix} 1 & 0 & 0 & 0 & 0 & 0 & 0 \\ 0 & 1 & 0 & 0 & 0 & 0 & 0 \\ 0 & -1 & 0 & 0 & 0 & 0 & 0 \\ 0 & 1 & 0 & 0 & 0 & 0 & 0 \\ 0 & 1 & 0 & 0 & 0 & 0 & 0 \\ 0 & -1 & 0 & 0 & 0 & 0 & 0 \\ 0 & 0 & 1 & 0 & 0 & 0 & 0 \\ 0 & 0 & 0 & 1 & 0 & 0 & 0 \\ 0 & 0 & 0 & 0 & 1 & 0 & 0 \\ 0 & 0 & 0 & 1 & -1 & 0 & 0 \\ 0 & 0 & 0 & 0 & 1 & 0 & 0 \\ 0 & 0 & 0 & 0 & 1 & 0 & 0 \\ 0 & 0 & 0 & 0 & -1 & 0 & 0 \\ 0 & 0 & 0 & 0 & 0 & 1 & 0 \\ 0 & 0 & 0 & 0 & 0 & 0 & 1 \end{bmatrix} \begin{bmatrix} q_{100,200} \\ q_{200,232} \\ q_{300,400} \\ q_{400,500} \\ q_{500,600} \\ q_{600,700} \\ q_{700,800} \end{bmatrix} + \begin{bmatrix} 0 \\ 0 \\ 0 \\ 0 \\ 0 \\ 0 \\ 0 \\ 0 \\ 0 \\ 0 \\ 0 \\ 0 \\ 0 \\ 0 \\ 0 \\ 0 \end{bmatrix}
$$

$$(14.1)$$

Numerical LCF of RECUPERA leg

The RECUPERA exoskeleton legs are each 7 DOFs with a 3 DOF ASPM representing the hip and ankle modules, and a 1 DOF prismatic joint that mimics the knee. A comprehensive kinematic analysis of ACTIVE ANKLE is provided in [13,21,22]. Since, it is not possible to get rotative inverse kinematics of the ASPM in a fully analytical fashion, the LCF of the ASPM modules in hip and ankle joints are resolved numerically.

Hybrid numerical-analytical LCF of overall RECUPERA system

Since, it is straight-forward to solve the inverse kinematics of STEWART–GOUGH PLATFORM, the overall LCF of the RECUPERA system can be achieved in a hybrid numerical-analytical manner using the approach defined in [23], where the arms (γ_2, γ_3) and torso (γ_1) submechanisms are solved analytically (using Eq. (14.1) for left and right arms) and the leg submechanisms (γ_4, γ_5) are solved numerically. The overall LCF of the RECUPERA system at position, velocity, and acceleration levels are given by Eqs. (14.2), (14.3), and (14.4), respectively.

$$\gamma = \begin{bmatrix} \gamma_1^T & \gamma_2^T & \gamma_3^T & \gamma_{4,num}^T & \gamma_{5,num}^T \end{bmatrix}^T \tag{14.2}$$

$$\mathbf{G} = \begin{bmatrix} \mathbf{G_1} & 0 & 0 & 0 & 0 \\ 0 & \mathbf{G_2} & 0 & 0 & 0 \\ 0 & 0 & \mathbf{G_3} & 0 & 0 \\ 0 & 0 & 0 & \mathbf{G_{4,num}} & 0 \\ 0 & 0 & 0 & 0 & \mathbf{G_{5,num}} \end{bmatrix} \tag{14.3}$$

$$\mathbf{g} = \begin{bmatrix} g_1^T & g_2^T & g_3^T & g_{4,num}^T & g_{5,num}^T \end{bmatrix}^T \tag{14.4}$$

Dynamics

Once the LCF of the overall system is available, the equations of motion of the explicitly constrained series–parallel hybrid system can be derived in both forward and inverse manners. The inverse dynamic model is solved in real time to enable torque control of the system.

14.3.3 Exoskeleton control

14.3.3.1 First level control

As described in Sec. 14.2.2, the first level control architecture for each joint is implemented on FPGAs, each driving a single actuator using a cascaded position, a velocity, and a current control loop. Each of the control cascades

can be directly selected for control. In Fig. 14.4, we can see the actuator level control architecture. With the help of motor current measurements, it is possible to use torque control for the motors. Further, the actuator level modularity enables the implementation of decoupled safety checks at the mid level controllers. Position, velocity and current are limited to a maximal value and in case of a sensor failure the controller is stopped automatically. This low-level architecture meets the requirements for the implementation of therapy concepts and teleoperation and is a solid foundation for both kinematic and dynamic control implemented in the mid-level architecture.

14.3.3.2 Mid-level control

The mid-level control architecture implements the kinematic and dynamic model of the system and associated control approaches for rehabilitation therapies and teleoperation. In the (1) *Gravity Compensation* (GC) mode, the weight of the system is compensated with the help of an inverse dynamic model of the exoskeleton arms. GC mode can also be used to take into account the dynamics of the human arms. The input to this model is the actuator positions read from the position encoders (see Table 14.3). The output is the reference torque values, which are then converted into motor current and sent to the current controller implemented in the ACU. The GC mode is used to implement a transparent behavior of the system and represents the *basic operation mode* of the system, on which most of the other modes are based on. Wrenches measured at the force-torque sensors of the exoskeleton arms can optionally be applied to assist human control of the exoskeleton. To support repetitive movement therapies for stroke patients, (2) *Teach & Replay* (TR) mode can be used. This mode has two phases: First, gravity compensation for the affected arm is enabled so that a therapist can easily move the arm. The equipped touch sensor on the forearm (see Fig. 14.3b) recognizes the intention of the therapist to teach a movement and stores the trajectory (position and velocity readings from the involved ACUs) in the system's storage device. Secondly, the trajectory can be replayed according to a trigger by the patient or therapist. During the replay, the exoskeleton executes the trajectory movement in the cascaded position-velocity control mode in the ACU. Additionally, mirror therapy is supported using the (3) *Mirror* (M) mode. Here, movements from the healthy arm can be transferred to the unhealthy arm in a mirrored fashion. In this mode, the healthy arm is gravity-compensated and the unhealthy arm is in cascaded position-velocity control mode. The actuator positions read from the healthy arm are mirrored and sent to the ACUs

of the unhealthy arm. Further, sitting and standing features for the lower part of the full-body exoskeleton are implemented at this level. As a new feature for telemanipulation, a robotic arm or the arms of a dual armed robot can be controlled using the (4) *Teleoperation* (TO) mode. The mapping between source system (exoskeleton) and target system (e.g., RH5 Manus) is done by a Cartesian mapping of the poses of selected end-effectors and can be scaled in Cartesian space. For that, a predefined pose mapping between end-effector frames is needed by adding additional links to the end-effectors in the URDF with a correcting transformation. For force feedback, the force-torque sensor wrenches at the target system are mapped to and applied at the corresponding frames of the source system. Wrenches can also be scaled and capped before they are applied to the exoskeleton. Additionally, the three trigger buttons on the left and right hand interfaces can be mapped to gripper joints.

14.3.3.3 High level control

A web-based GUI is provided for high level control of the exoskeleton and can be accessed using a mobile phone, tablet or PC. The web server is hosted on ZynqBrain2 and based on the Python Flask framework [24]. The GUI allows the user/therapist to select the operation mode of the exoskeleton, which can be either one of the different therapy modes (GC, M, or TR) or the TO mode. It is also possible to manage different patient/operator profiles storing specific information like ID or recorded movements. As the exoskeleton can be adjusted to the user, shoulder width, upper arm length, forearm length and hand size values can be entered in the GUI to automatically create the corresponding user-specific URDF files with the adjusted segment lengths and inertia using Phobos. Moreover, it allows the operator to use the exoskeleton in different settings: single arm, dual arm, full body, etc. Both left and right sided users can be supported. For the TO mode, force feedback can be manually activated and capped. As force feedback changes the poses of the exoskeleton hand interfaces, which in return changes the mapped end effector poses of the teleoperated robot, it is also possible to disable position control, so that the operator can have force feedback without changing the target system.

14.3.3.4 Software design

The high- and mid-level control is implemented using the Robot Construction Kit (Rock) [25]. It is based on the component model of the Orocos Real Time Toolkit (RTT) and an object request broker (ORB)
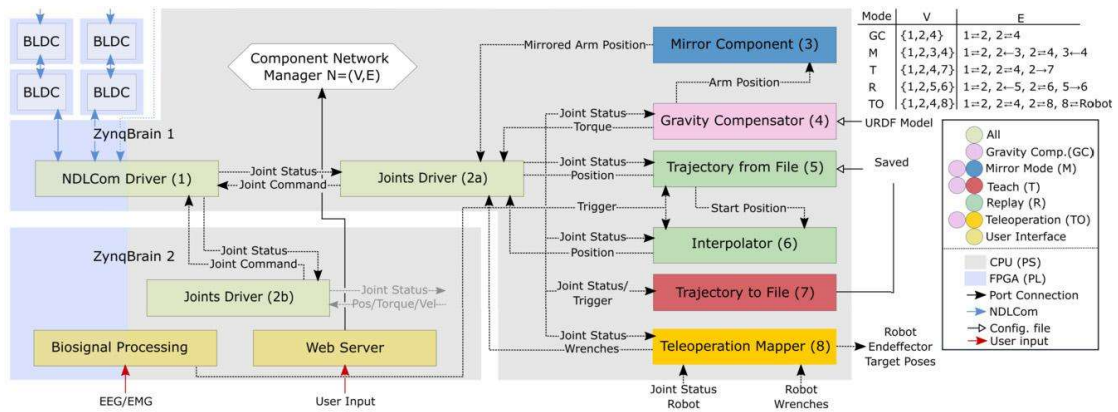
Figure 14.7 Software architecture overview: A Component Network Manager configures, connects and starts the subset of components (V) required for a specific mode. The corresponding directed connections (E) are described in the table at the top right corner. The components required for each mode are also represented by colors. A web server application hosted on ZynqBrain 2 is used as user interface.

implementation called omniORB. Rock tasks, similar to ROS (Robot Operating System) nodes, encapsulate different functionalities, run independently and provide input and output for other tasks (see Fig. 14.7). Each task can be configured individually. This enables a very flexible way to adjust the system and to distribute computational demanding components among the two ZynqBrains. Additionally, a web server is running on the second ZynqBrain, providing access to the previously described web GUI written in JavaScript (see Section 14.3.3.3). Furthermore, some functionalities can be triggered by biosignals like electroencephalogram (EEG) or electromyogram (EMG), which can be processed directly on the embedded processors [3,17].

14.4 Results and discussion

This section presents the experimental results of the rehabilitation therapy modes and the teleoperation implemented in the wheelchair configuration. The rehabilitation modes were also tested in clinical settings with affected individuals, see [26]. Since the upper body design is identical for both configurations, the results are equally valid between them. Further, we present a comparison with current state of the art exoskeletons for rehabilitation and teleoperation purposes.

14.4.1 Gravity compensations mode

Transparency of the exoskeleton to the user requires a good gravity compensation model, which is also needed for a good usability for the therapist. In our experiments, described in [22], the norm of mean absolute error (MAE) in joint space of four different balanced poses was between 0.12 Nm & 0.26 Nm, which demonstrates the good quality of the model. In the experiments, the exoskeleton user was able to move its arms freely within the limits of the system, as depicted in Fig. 14.8a. When using the gravity compensation mode, it is also possible to include the weight of the human arms into the model for compensation. Additionally, gravity compensation mode is being used for the get-in helper mode, enabling the human operator or patient to easily enter the exoskeleton. This can be done in less than a minute on average for healthy users if no adjustments to the system are needed.

14.4.2 Rehabilitation
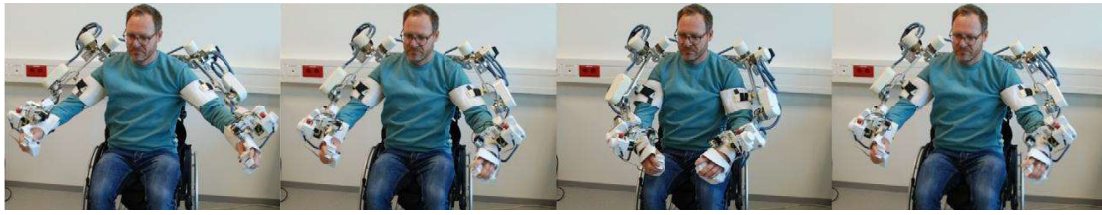
14.4.2.1 Teach and replay

The teach and replay mode gives a therapist the possibility to pre-train movements and later replay these as a sequence or individually. The patient can benefit from a self-intended movement start, since the replay of a pre-trained movement can be triggered via residual muscle activity measured with surface EMG and thus give the patient the possibility to train self-paced, shown in Fig. 14.8b.

14.4.2.2 Mirror mode

The mirror mode mimics a mirror therapy by directly transferring movements from the healthy arm to the affected one. In this mode, the non-affected arm controls or moves the exoskeleton in the gravity compensation mode. All movements are mirrored to the affected side which is running in the position control mode (see Fig. 14.8c). With this mode, the patient is able to do self-determined training.

14.4.2.3 Gravity compensation with human arm model

As an addition to the pure gravity compensation mode, the weight of the arm of the user can be modeled as well. In this way, only very small residual muscle force is sufficient to move the affected arm. This mode gives patients the opportunity to do self-paced training of voluntary movements, without

(a) Gravity Compensation Mode: base mode for mechanical transparency.

(b) Teach and Replay Mode: recorded movements are replayed.

(c) Mirror Mode: all movements are mirrored from the right to the left side.

**Figure 14.8** Selected modes of exoskeleton use.

any constraints like in the other modes where the movements are pre-trained or mirrored from the non–affected side.

14.4.3 Teleoperation

In teleoperation mode, we are able to remotely control both the arms of our humanoid robot RH5 MANUS. The elbow and wrist poses of the exoskeleton were mapped to RH5 MANUS, while wrenches measured at the force-torque sensors in the wrists of the humanoid were applied at corresponding links of the exoskeleton. Using the trigger buttons at the hand interfaces, the fingers of the two-finger and four-finger grippers could be controlled independently. With this setup, it was possible to grasp and pick up an object with one hand, rotate it and then put it back on a table (see Fig. 14.9).

   In further tests, we were also able to grasp an object like a box or a soft ball with both hands at the same time. For this, we did not use the fingers to grasp the object, but used the hands for contact.
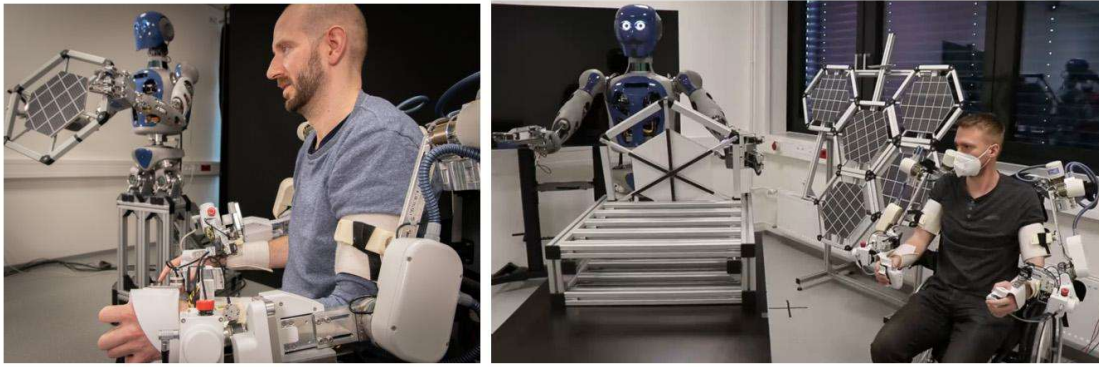
Figure 14.9 Exoskeleton teleoperating RH5 Manus.

In all our teleoperation tests, Cartesian workspace scaling has proven to be a helpful tool, especially for robots with different workspaces than the exoskeleton. Workspace scaling can also be used to scale down the human movement and therefore enable a very precise pose control. Also, the scaling can be chosen according to the current task.

14.4.4 Comparison with similar exoskeleton systems

A classification of the exoskeleton can be done by featuring active DOF, ROM, mobility, number of tracked limbs and weight. A comparison with similar upper body exoskeleton systems in Table 14.4 shows that the Recupera upper body exoskeleton has the best lightweight design. The Recupera exoskeleton is a mobile system mounted to a commercially available wheelchair. It has a high amount of active DOFs with a low weight. The total weight of an arm after enhancing the system to active 7 DOF is 7.14 kg. This also includes an active hand interface for teleoperation. By modifying the arms, the ROM of the elbows and forearms was significantly increased. Although it does not cover the complete human workspace, it supports most activities of daily living tasks. The alternative inclusion of an active shoulder girdle would have increased shoulder ROM to achieve full working range, but would also have limited design complexity and thus mobility. In the full-body system, the total working range of the arms is increased by the active back. The active back and legs enable rehabilitation therapies of the upper body in sitting as well as in standing.

Table 14.4 Comparison of updated RECUPERA upper-body system to other upper-body exoskeletons and the range of motion of activities of daily living.

Device	RECUPERA	ANYexo [27]	Harmony [11]	SUEFUL-6 [28]	ADL [11,29,30]
Weight (kg)	14.3	12.98	31.2	–	–
DOF	14	7	14	6	–
Bilateral	yes	no	yes	no	–
Torso harness	yes	no	yes	no	–
Gripper	yes	no	no	no	–
Wheelchair	yes	no	no	yes	–
Abd./Adduction °(Nm)	87/40(28)	170/0(40)	170/60(34)	–	131/54
Ex./Int. rot. °(Nm)	40/75(18)	105/105(40)	79/80(34)	0/90(35)	76/62
Flex./Ext. °(Nm)	170/30(28)	170/50(40)	160/45(34)	0/90(9)	131/51
Elbow flex. °(Nm)	145(18)	145(40)	150(13)	120(9)	148
Pro/supinat. °(Nm)	176(7.1)	–	172(1.25)	140(4)	167
Wrist Abd./Add. °(Nm)	20/40(3.4)	–	–	20/30	30/40
Wrist Flex./Ext. °(Nm)	43/43(3.4)	–	–	60/50	60/60

14.5 Conclusion and outlook

The RECUPERA exoskeletons are two modular, lightweight, safe and ergonomically adaptable robotic systems that serve to capture and guide human movement. The upper-body part system attached to a wheelchair, as a partial variant of the full-body system, reduces complexity and transfers its own weight to the floor via the wheelchair. However, the full-body system supports its own weight and enables a wider range of movement due to an active back. The active legs enable a sitting posture through an extendable seat mechanism. Both systems can be used for rehabilitation applications and for teleoperation. Since the systems are designed as rigid exoskeletons, the range of motion and system dynamics must be optimally suited for mechanical transparency for the user. This applies to both teleoperation and rehabilitation applications. Here, further improvements can be made. The mechanical components can be optimized with regard to medical-technical specifications. In order to increase the system dynamics, a change to drives with a reduced gear reduction could be considered.

The RECUPERA exoskeleton was used in two application scenarios. Using gravity compensation mode as a basic function, the exoskeleton is self-supporting and allows free movement of the user. The humanoid robot RH5 MANUS was remotely controlled. Through the exoskeleton a haptic impression of the object manipulation was given using force feedback. Additionally, Cartesian workspace scaling enables a precise remote control. When manipulating an object similar to a ring using a dual arm power grasp, this introduced a kinematic closed loop of both the arms, which were now connected through the object. Due to latencies introduced by the two systems, the interaction forces of the two arms with the object and therefore with the other arm could not be compensated by the human operator and the system was rocking up. Additional tests with activated compliance mode for the wrists at mid-level control of RH5 MANUS reduced this effect. Further research needs to be done in this direction to enable dual arm power grasping.

As a rehabilitation application, mirror therapy and EMG triggered Teach & Replay mode as well as the arm weight compensation model were tested with patients. It was observed that depending on the severity of the patient's restriction different modes were supporting rehabilitation therapy best.

The assist-as-needed technique in assistive robotic rehabilitation has proven to promote motor recovery and induce neuroplasticity by encouraging the patient to actively participate in the movements [31]. This is in stark contrast to the above discussed Teach & Replay and Mirror modes, where the exoskeleton does the entire work. To deviate from this and give the patient full control of initiating and executing these movements up to their current capabilities, this technique will be integrated into the exoskeleton design in the near future. In essence, this technique encourages the patient to carry out movements depending upon their muscular ability and assistance will be provided only when they are deviating significantly from the desired trajectory to guide them towards the target.

To this end, the task is divided into three categories – initial calibration, online estimation of muscle torques and assistive control. In the calibration phase, Maximum Voluntary Isometric Contraction would be used to generate a preliminary estimate of muscle strength. Promising progress has been made in real-time estimation of the joint torques using the EMG signals. Several experiments have been conducted at DFKI in this regard wherein this mapping has been achieved for single joint force using a linear regression model and for multiple joints using a two-layer artificial neural

network model, for which further improvements and validations are still needed. The results will be published in the near future.

Furthermore, to ensure that the patient is provided with a free zone around the desired trajectory, a tunnel-based torque controller is planned to be implemented. As the performance of the controller depends on the accuracy of the inverse dynamic model, it forms a major bottleneck and its quality needs to be further investigated in the future.

References

[1] F. Just, Ö. Özen, P. Bösch, H. Bobrovsky, V. Klamroth-Marganska, R. Riener, G. Rauter, Exoskeleton transparency: feed-forward compensation vs. disturbance observer, at-Automatisierungstechnik 66 (12) (2018) 1014–1026.

[2] R. Gopura, D. Bandara, K. Kiguchi, G.K. Mann, Developments in hardware systems of active upper-limb exoskeleton robots: a review, Robotics and Autonomous Systems 75 (2016) 203–220.

[3] E.A. Kirchner, N. Will, M. Simnofske, L.M.V. Benitez, B. Bongardt, M.M. Krell, S. Kumar, M. Mallwitz, A. Seeland, M. Tabie, H. Wöhrle, M. Yüksel, A. Heß, R. Buschfort, F. Kirchner, Recupera-Reha: exoskeleton technology with integrated biosignal analysis for sensorimotor rehabilitation, in: Transdisziplinäre Konferenz SmartASSIST, 2016, pp. 504–517.

[4] E.A. Kirchner, J. Bütefür, Towards bidirectional and coadaptive robotic exoskeletons for neuromotor rehabilitation and assisted daily living: a review, Current Robotics Reports 3 (2022) 21–32.

[5] K.J. Miller, A. Gallina, J.L. Neva, T.D. Ivanova, N.J. Snow, N.M. Ledwell, Z.G. Xiao, C. Menon, L.A. Boyd, S.J. Garland, Effect of repetitive transcranial magnetic stimulation combined with robot-assisted training on wrist muscle activation post-stroke, Clinical Neurophysiology 130 (8) (2019) 1271–1279, https://doi.org/10.1016/j.clinph.2019.04.712.

[6] A.U. Pehlivan, D.P. Losey, M.K. O'Malley, Minimal assist-as-needed controller for upper limb robotic rehabilitation, IEEE Transactions on Robotics 32 (1) (2016) 113–124, https://doi.org/10.1109/TRO.2015.2503726.

[7] M. Folgheraiter, M. Jordan, S. Straube, A. Seeland, S.K. Kim, E.A. Kirchner, Measuring the improvement of the interaction comfort of a wearable exoskeleton, International Journal of Social Robotics 4 (3) (2012) 285–302.

[8] M. Mallwitz, N. Will, J. Teiwes, E.A. Kirchner, The CAPIO active upper body exoskeleton and its application for teleoperation, in: Proceedings of the 13th Symposium on Advanced Space Technologies in Robotics and Automation (ASTRA-2015), ESA, 2015.

[9] R. Sonsalla, F. Cordes, L. Christensen, T.M. Roehr, T. Stark, S. Planthaber, M. Maurus, M. Mallwitz, E.A. Kirchner, Field testing of a cooperative multi-robot sample return mission in Mars analogue environment, in: Proceedings of the 14th Symposium on Advanced Space Technologies in Robotics and Automation (ASTRA), 2017.

[10] M. Boukheddimi, S. Kumar, H. Peters, D. Mronga, R. Budhiraja, F. Kirchner, Introducing RH5 Manus: a powerful humanoid upper body design for dynamic movements, in: 2022 International Conference on Robotics and Automation (ICRA), IEEE, 2022, pp. 01–07.

[11] B. Kim, A.D. Deshpande, An upper-body rehabilitation exoskeleton harmony with an anatomical shoulder mechanism: design, modeling, control, and performance evaluation, The International Journal of Robotics Research 36 (4) (2017) 414–435.

[12] S. Kumar, B. Bongardt, M. Simnofske, F. Kirchner, Design and kinematic analysis of the novel almost spherical parallel mechanism active ankle, Journal of Intelligent & Robotic Systems 94 (2019) 303–325, https://doi.org/10.1007/s10846-018-0792-x, https://link.springer.com/article/10.1007/s10846-018-0792-x#citeas.

[13] M. Simnofske, S. Kumar, B. Bongardt, F. Kirchner, Active ankle – an almost-spherical parallel mechanism, in: 47th International Symposium on Robotics (ISR), 2016.

[14] M. Zenzes, P. Kampmann, T. Stark, M. Schilling, NDLCom: simple protocol for heterogeneous embedded communication networks, in: Proceedings of the Embedded World Exhibition & Conference, Nuremberg, Germany, 2016, pp. 23–25.

[15] iC-MU Magnetic Off-Axis Absolute Position Encoder, http://www.ichaus.de/ic-mu.

[16] Xilinx Inc., UG585 Zynq-7000 All Programmable SoC Technical Reference Manual, 1st edition, February 2015.

[17] H. Wöhrle, M. Tabie, S.K. Kim, F. Kirchner, E.A. Kirchner, A hybrid FPGA-based system for EEG- and EMG-based online movement prediction, Sensors 17 (7) (2017), https://doi.org/10.3390/s17071552.

[18] M. Yüksel, L.M.V. Benitez, D. Zardykhan, F. Kirchner, Mechatronical design and analysis of a modular developed exoskeleton for rehabilitation purposes, in: 10th International Conference on Electrical and Electronics Engineering (ELECO), 2017, pp. 711–716.

[19] Solidworks to URDF exporter, http://wiki.ros.org/sw_urdf_exporter. (Accessed 30 September 2022).

[20] S. Kumar, M. Simnofske, B. Bongardt, A. Müller, F. Kirchner, Integrating mimic joints into dynamics algorithms: exemplified by the hybrid Recupera exoskeleton, in: Proceedings of the Advances in Robotics, AIR '17, ACM, New York, NY, USA, 2017, pp. 27:1–27:6, https://doi.org/10.1145/3132446.3134891.

[21] S. Kumar, A. Nayak, B. Bongardt, A. Mueller, F. Kirchner, Kinematic Analysis of Active Ankle Using Computational Algebraic Geometry, Springer International Publishing, Cham, 2018, pp. 117–125.

[22] S. Kumar, H. Wöhrle, M. Trampler, M. Simnofske, H. Peters, M. Mallwitz, E.A. Kirchner, F. Kirchner, Modular design and decentralized control of the Recupera exoskeleton for stroke rehabilitation, Applied Sciences 9 (4) (2019).

[23] R. Kumar, S. Kumar, A. Müller, F. Kirchner, Modular and hybrid numerical-analytical approach – a case study on improving computational efficiency for series–parallel hybrid robots, in: IEEE/RSJ International Conference on Intelligent Robots and Systems (IROS) 2022, 2022.

[24] FLASK, web development one drop at a time, http://flask.pocoo.org/.

[25] ROCK, the Robot Construction Kit, http://www.rock-robotics.org.

[26] Recupera-Reha exoskeleton first patient test, suffering from a right sided paralysis after stroke, https://www.youtube.com/watch?v=2Llq63VEFRg. (Accessed 6 October 2022).

[27] Y. Zimmermann, A. Forino, R. Riener, M. Hutter, ANYexo: a versatile and dynamic upper-limb rehabilitation robot, IEEE Robotics and Automation Letters 4 (4) (2019) 3649–3656.

[28] R.A.R.C. Gopura, K. Kiguchi, Development of a 6DOF exoskeleton robot for human upper-limb motion assist, in: 2008 4th International Conference on Information and Automation for Sustainability, 2008, https://doi.org/10.1109/ICIAFS.2008.4783986.

[29] D. Magermans, E. Chadwick, H. Veeger, F. Van Der Helm, Requirements for upper extremity motions during activities of daily living, Clinical Biomechanics 20 (6) (2005) 591–599.

[30] H. Schmidtke, I. Jastrzebska-Fraczek, Ergonomie: Daten zur Systemgestaltung und Begriffsbestimmungen, Carl Hanser Verlag GmbH & Company KG, 2013.

[31] S.Y.A. Mounis, N.Z. Azlan, F. Sado, Assist-as-needed control strategy for upper-limb rehabilitation based on subject's functional ability, Measurements & Control 52 (9–10) (2019) 1354–1361.